Universitat Politècnica de Catalunya (UPC)
Universitat Autònoma de Barcelona (UAB)
Universitat de Barcelona (UB)
Institut de Ciències Fotòniques (ICFO)

http://www.photonicsbcn.eu

Master in Photonics

MASTER THESIS WORK

Spatial beam manipulation by Photonic Crystal

Jorge Luis Basurto Zapana

Supervised by Dr. Kestutis Staliunas, (UPC-Terrassa)

Presented on date 8th September 2014

Registered at

Escola Tècnica Superior d'Enginyeria de Telecomunicació de Barcelona

Spatial beam manipulation by Photonic crystal

Jorge Luis Basurto Zapana
Group of Nonlinear Dynamics, Nonlinear Optics and Lasers, Departament de Física i Enginyeria Nuclear, Universitat Politècnica de Catalunya, Campus de Terrassa, Terrassa 08022, Spain

E-mail: jluisb7@gmail.com

Abstract. Photonic crystals are as promising materials for controlling and manipulating the flow of light. In this work we investigate different aspects of narrow beam propagation through the photonic crystals by theoretical analysis and numerical simulations. We present such aspects of beam propagation as the double focalization, the dependence of focusing on frequency, and the effects of a limited numerical aperture of this lens. Specifically we simulate a photonic crystal made of glass with periodic structures of square and triangular symmetries.

Keywords: Photonic crystal, bands, k-space, focusing, numerical aperture.

1. Introduction

Photonic crystals (PhCs) are dielectric materials with a periodic structure, i.e. with periodically a varying refraction index on a wavelength scale. Such structures have been theoretically studied since long time ago, and the studies strongly intensified recently, the last two decades, when the fabrication of such structures become possible. The technologies required for its manufacture have been developed and improved, and now the fabrication of the periodic nanoscale structures with high precision is possible, allowing the manufacture of one-dimensional (1D), two-dimensional (2D) and three-dimensional (3D) photonic structures.

The theoretical analysis starts from the Maxwell equations with a spatial dependence in the electric permittivity $\varepsilon(\vec{r})$. The Maxwell equations typically result to the wave equation for this system.

$$\vec{D} = \varepsilon_0 \varepsilon(\vec{r})\vec{E} \qquad \frac{1}{\varepsilon(\vec{r})}\vec{\nabla}^2\vec{E} - \frac{1}{c^2}\frac{\partial^2}{\partial t^2}\vec{E} = 0 \tag{1}$$

The analysis of this equation yields a certain similarity with the equations of quantum mechanics, and therefore we can solve this equation mathematically using the eigenvalues and eigenvectors. Another important point is the relations with solid state physics where the atoms or molecules are distributed periodically and therefore they obey a discrete translational symmetry, the PhC reflects the same symmetry i.e. we define a lattice constant as a constant vector that gives the distance at which the pattern of the solid or PhC repeats.

If we perform an analysis of (1) in a similar way as in a solid (crystalline) material, it is possible obtain a graph of $\omega(k)$ that has different bands analogous to the energy bands in the solid materials. Similarly to the approach in solid state physics it is also possible to have a Brillouin Zone and unitary cell in the PhC.

In particular we obtain the gaps where, for some frequencies, the real wave vector does not exist (the solution is a complex wavevector). At these frequencies, the beam is totally reflected from the semi-infinite PhC, or is partially transmitted as evanescent wave through the slice of PhC of finite width.

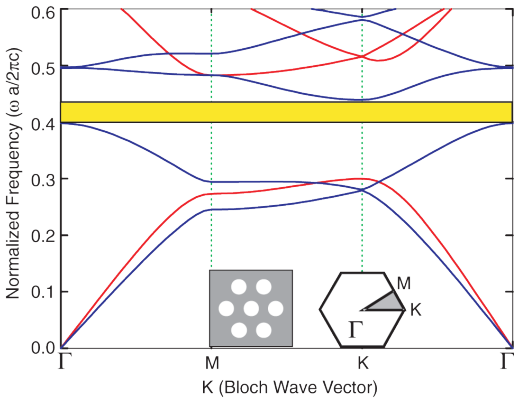

Figure 1. Band diagram and irreducible Brillouin Zone the some structure represented in the graph. The yellow line represents the band gap. The structure considered is of hexagonal symmetry.

In the iso-frequency graphs the direction of the vector 'k 'is the direction of the wave phase velocity. The group velocity of the wave is defined by:

$$\vec{v}_g = \frac{\partial \omega}{\partial \vec{k}} \tag{2}$$

Besides providing us with this information, the group velocity of the wave tells us the points where nonlinear dispersion occurs, implying that at these points the effective refractive index is greater. This is important for the control of optical signals in the time domain.

As seen in the graph, the first graph iso-frequency (Fig 2 (a)) is produced by a homogeneous medium, and shows how the beam propagates through space, that is, if we project the vectors 'k' on the z axis is the direction of propagation, we see a different delay for each relative vector 'k'. The delay phase shows how the wave spreads as shown in the figure below (Fig 2 (a)).

In the second case we see that the spatial dispersion in the PhC has a part that is completely flat (Fig 2 (b)). This implies that we project all vectors 'k' in the z direction; we didn't observe any phase shift between them. This is very important because this can make a wave to suffer no diffraction when passing through. This material, as one can see in the figure below (Fig 2 (b)), is a field of research that studied the propagation of light over long distances without loss for diffraction and following a fairly flat course. This type of behavior in a PhC is called non-diffractive propagation of a light beam or self-collimation [2-4, 6].

The last graph illustrates the case of iso-frequency curve with a convex shape (Fig 2 (c)). We can see the phase delay occurring in the central components of the wave. In this case the diffraction is still present in the displacement of the wave, but the wave front is convex in shape as seen in the figure below (Fig 2 (c)).

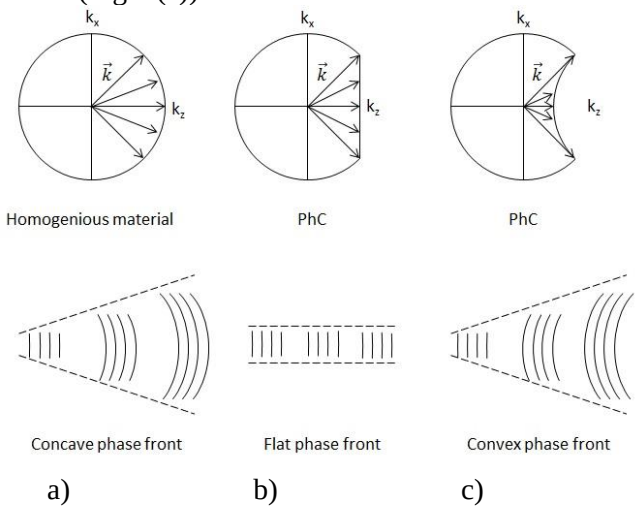

Figure 2. Illustration of iso-frequency contour and of the wave fronts of the beam in propagation through homogeneous material (a), the PhC without diffraction (b) and the PhC with negative diffraction (c).

To create a flat lens with a photonic crystal we need that at a certain frequency the iso-frequency graph is to be convex. In front of the PhC, in air, the beam is normally diffracted until enters into PhC which creates a negative diffraction which causes the beam to come together to achieve a flat beam then continues to spread with negative diffraction until the exit of the PhC. When the beam exit to PhC we have positive diffraction again, which at some distance (the focal distance) compensates the diffraction in the PhC, and we have a focused beam which then continues to spread with positive diffraction [7-9].

2. Simulation of flat lensing

For the simulations we used 2D PhC with two different symmetries of structures, both periodic, in a photonic crystal of the same dimensions (Fig 3). Specifically the simulated PhC is of a transverse length $L_x = 50\mu m$ and a width $L_z = 10\mu m$.

The refractive index of the dielectric cylindrical rods of the structure are $n = 1.5$ of radius $R = 0.2\mu m$. Both structures have a lattice constant equal to $a = 0.7\mu m$ and the host material is air.

The first structure to be simulated is a square structure with an angle $\alpha = 90°$ and the second simulated structure is an equilateral triangular structure with an angle $\alpha = 60°$.

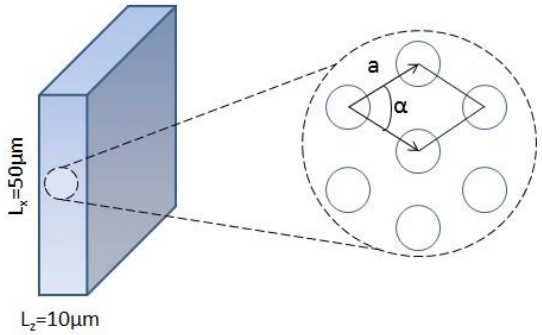

Figure 3. Photonic crystal with transverse length equal to L_x = 50μm and width equal to L_z = 10 μm, where the lattice constant is equal to a = 0.7 μm and the radius of rods is R = 0.2 μm. The angle depends if we have a square or rhombic structure where the angle is equal to α = 90º or if the structure is an equilateral triangle α = 60º.

The important aspects to be analyzed are the spatial dispersion diagrams or iso-frequency plots for to see if is possible to obtain focus as we saw above.

For the square structure the iso-frequency diagrams are shown in Fig 4. The first diagram shows the iso-frequency of the first photonic band where the arrows indicate the direction in which the beam moves when it passes through these iso-frequencies which it's obeys the Equation 2.

In the first photonic band for a/λ = 0.05 (λ = 14μm) - a/λ = 0.35 (λ = 2μm) the beam has a positive diffraction like a homogeneous medium and therefore for these wavelengths we don't have a focusing point. If a/λ increase the curve goes to a flatter curve, when the values of a/λ are near to a/λ = 0.45 is possible to obtain a flat curve where in this point the beam don't have diffraction. If we continuous increase the values of a/λ we arrive a one point where the surface having a convex shape, these values of a/λ with this convex shape goes to a/λ = 0.47 (λ = 1.49μm) more or less to a/λ = 0.55 (λ = 1.27μm), for these wavelengths can be obtained focalization and therefore we have a flat lens.

In the second photonic band the direction of velocity group goes to outside of the graph to the center of the graph because the gradient of frequency has this direction. In this second photonic band we see that for small values of a/λ we don't see anything important. When the values of a/λ are near to a/λ = 0.65 (λ = 1.077μm) appears a iso-frequency curves with convex shape but these shape are not very spherical they have a shape similar to rhomboidal form, for this reason the focusing point generated by these curves have elongated shape.

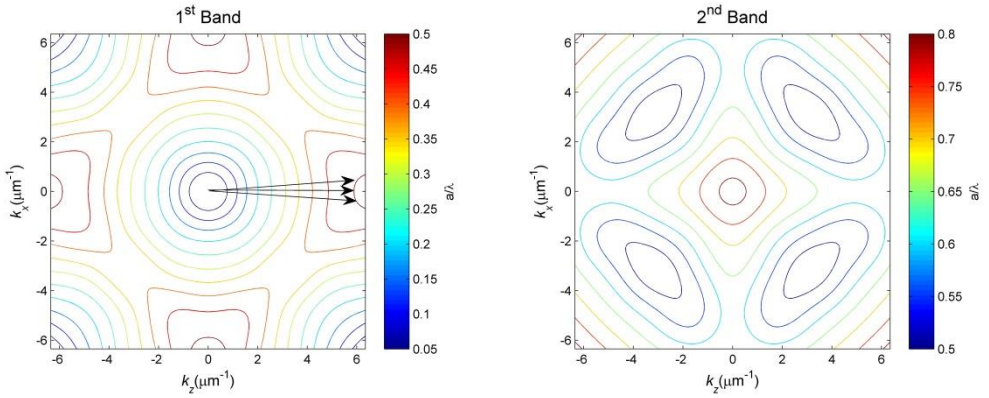

Figure 4. First and second photonic band that shows a iso-frequency curves generated for square shape. The arrows show the direction towards which the group velocity moves or the gradient of these bands.

For the triangular structure, the first photonic band shows a similar behaviour as the above structure, the iso-frequency curves have a concave form in almost all bands and for this the beam is diffracted positively like a normal medium. The interesting behaviour we see in the second photonic band, in this band the group velocity goes to the centre to the graph. For values of a/λ = 0.55 (λ = 1.27μm) - a/λ = 0.6 (λ = 1.16μm) we have a positive diffraction. When the values of a/λ increase (a/λ = 0.7 (λ = 1μm) - a/λ = 0.725 (λ = 0.96μm)) we see that the iso-frequency curve is transformed into a flatter curve that generates a beam without diffraction.
For values of a/λ = 0.75 (λ = 0.93μm) or less we start to see that the iso-frequency curve it start to have a convex form and the beam have a negative diffraction and it is possible to obtain a focusing point. We can see that for values of a/λ around a/λ = 0.8 (λ = 0.875μm) - a/λ = 0.9 (λ = 0.77μm) the iso-frequency curve have more spherical form and is more easy to see a focal point.
In the third photonic band the group velocity it has a direction to the centre of the graph and we see that for values of a/λ smallest we don't see anything interesting in the middle of the band, but for values of a/λ between a/λ = 0.85 (λ = 0.824μm) - a/λ = 0.9 (λ = 0.77μm) we have a convex curve and the beam it has a negative diffraction and is possible to obtain a focusing point where the more clear focusing point is when a/λ is equal to a/λ = 0.9 (λ = 0.77μm).

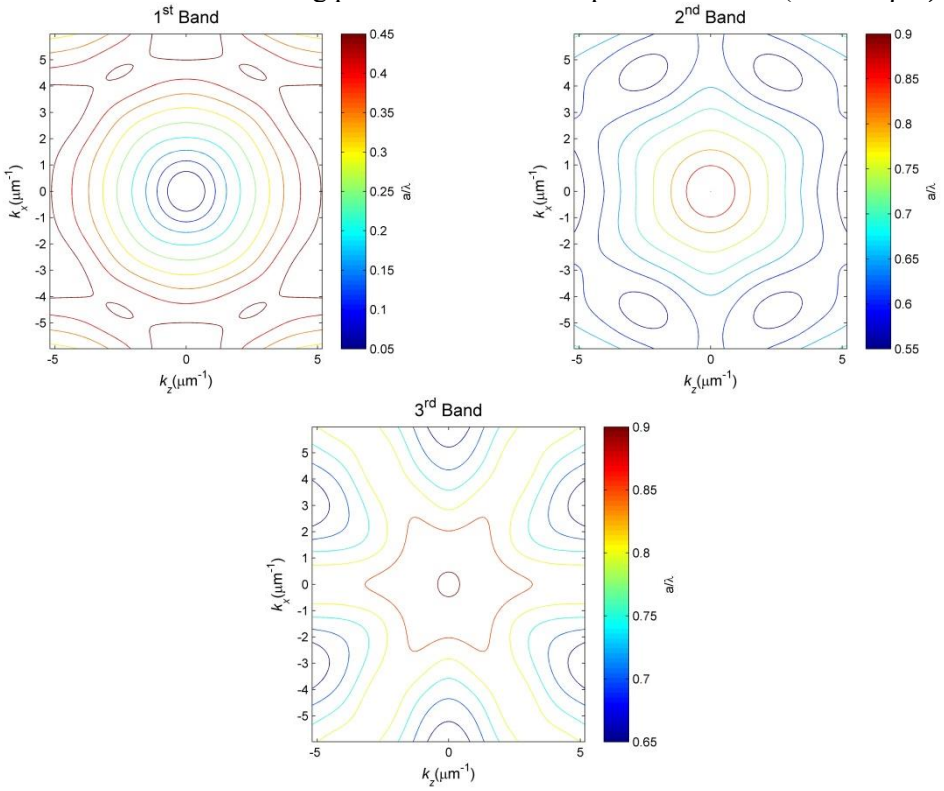

Figure 5. First, second and third iso-frequency curves generated for triangular shape.

In the latter structure we can see that for values of a/λ between a/λ = 0.85 (λ = 0.824μm) - a/λ = 0.9 (λ = 0.77μm) is possible to obtain a focusing points in two different photonic bands, this is interesting because it means that for a same region of value of a/λ the second and third band overlap and therefore that the different portions of radiation for the same frequency a/λ will project to these different curvatures and obtain two different focal positions for the same frequency, the name for this behavior is double focusing (Fig 6)[1].

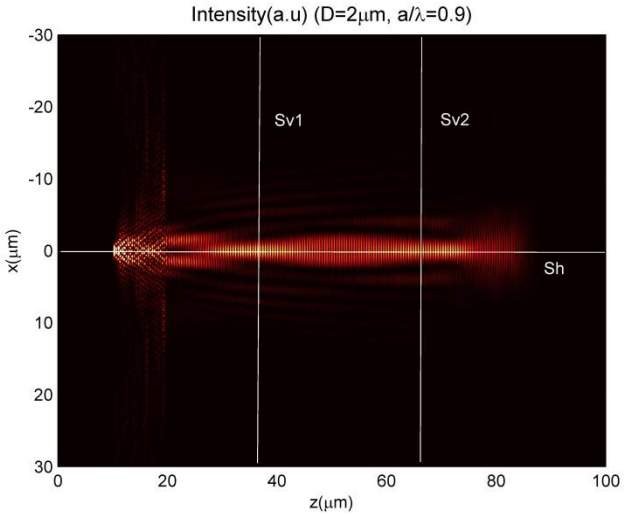

Figure 6. Simulation image where shows a double focusing where Sv1, Sv2 and Sh are a sensors. The width of the incident beam is D=2μm. We can see that the first focusing point is approximately in position z=35μm and the second is in z=70μm.

An important aspect in the analysis of focusing for a PhC is the relation between the focusing distances and the focal length. In a conventional lens the relation between the focal length and the distances from the lens to focal point is equal:

$$\frac{1}{f} = \frac{1}{l_1} + \frac{1}{l_2} \tag{3}$$

Where f is a focal length, l_1 is a distance from the object plane to the lens and l_2 is a distance from the image plane to the lens. But for PhC, where we have flat, near field lensing, the relation for the focal length is different:

$$f = l_1 + l_2 \tag{4}$$

The important difference is that the Equation 4 is clearly linear and cannot result into infinite distance of image. Other important aspect is that the optical axis is absent [10] i.e. the PhC is invariant in the lateral direction (apart from the small scale periodicity) (Fig 7).

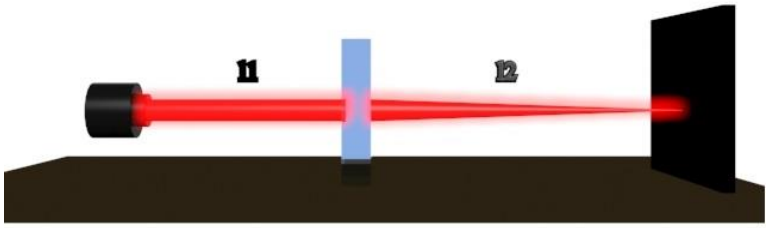

Figure 7. Flat PhC lensing scheme. Where l_1 is the distance from the output beam of the laser to the input of the beam in PhC and l_2 is the distance from the output beam of PhC to the focal point.

We prove this behavior (the relation (4)) by simulating our structures. In the square structure we see that when the distance of focal point (l_1) increase the distance behind the crystal (l_2) decrease linearly (Fig 8 (a)). The slope is not exactly equal to -1 as predicted for Equation 4,

which can be attributed to a finite size of the crystal, and other discrepancies from the idealized conditions. In the triangular structure we see the same behavior l_2 decrease when l_1 increase, but in this case the slope is very close to -1 as can be seen on the white line in Figure 8 (b). Also is possible to see the double focusing points and how both focusing points moves linearly.

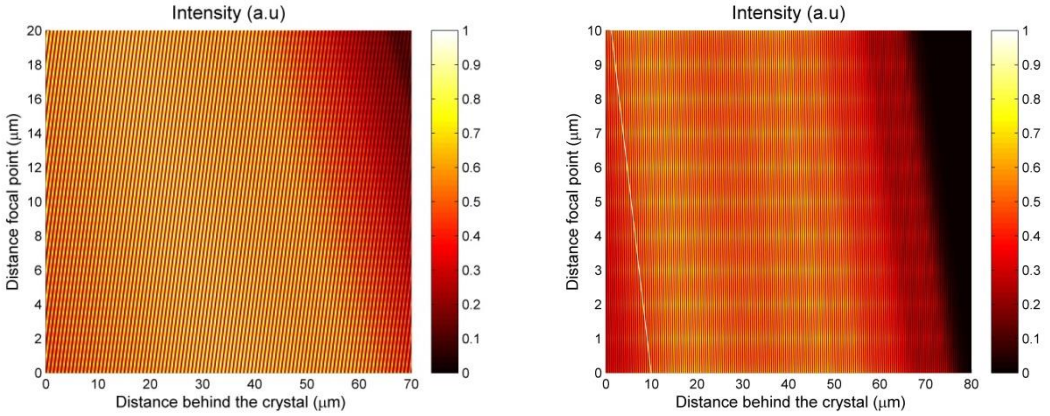

a) b)

Figure 8. Distance behind the crystal (l_2) behaviour when increase the distance of focal point (l_1) for square structure (a) and triangular structure (b). We can see the linear behaviour but the square structure have a slope different to -1 how predict the Equation 4 and the triangular structure is near to -1 (white line). Also in (b) is possible to see clearly the positions focal points because we have double focusing in $l_2 \cong 15\mu m$ and $l_2 \cong 50\mu m$.

3. Focusing distance depending on the frequency

Now for the different structures we analyzed the graphic representation of frequency in function of distance behind the crystal. In the Figure 9 we see the band diagram of square structure, but in this diagram the important part is the ΓX direction because is the direction in which we propagate the beam. In this part we see that we have a band gap at frequencies $a/\lambda \cong 0.5$ from $a/\lambda \cong 0.6$. And in the graph of frequency in function of distance is possible to see this gap, we can see that for values bigger than $a/\lambda \cong 0.5$ we don't obtain more intensity and for values near to $a/\lambda \cong 0.5$ we see almost nothing of intensity.

Also is possible to see the focusing point for $a/\lambda = 0.5$ how we saw in the previous part. For values of $a/\lambda = 0.4$ - $a/\lambda \cong 0.5$ we see the part where appear the nondiffractive behavior predicted for the first iso-frequency diagram (Fig 4). And for values near to $a/\lambda \cong 0.6$ is possible to see a focusing point but this point is very diffusing and bad for work with this.

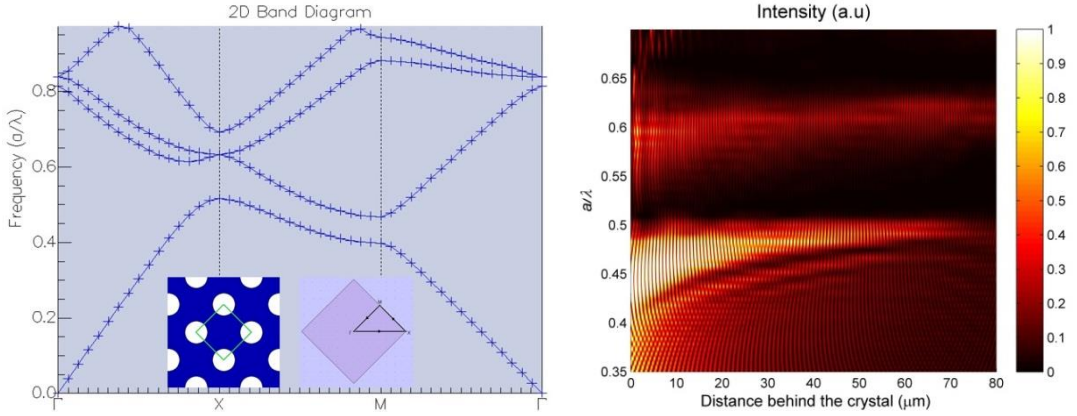

Figure 9. Photonic band diagram for square structure and in small, the structure and Brillouin Zone. Representation of frequencies in function of distance behind the crystal at x=0.

For triangular structure the important part is the ΓX direction. We can see in the band diagram the point where the bands overlap, this point is a/λ = 0.9 and in this point is possible to obtain a double focusing how we saw in the previous part. In the frequency in function of distance map we see that a great part we have a nondiffractive beam (a/λ ≅ 0.75 - a/λ ≅ 0.8) how it was predicted in the iso-frequency diagrams. And for bigger values we have a focusing points (a/λ ≅ 0.8 - a/λ ≅ 0.85). In this graph is not possible to see the double focusing point at a/λ = 0.9 because how we will see in the next part the width of the input beam do possible to see or not a double focusing.

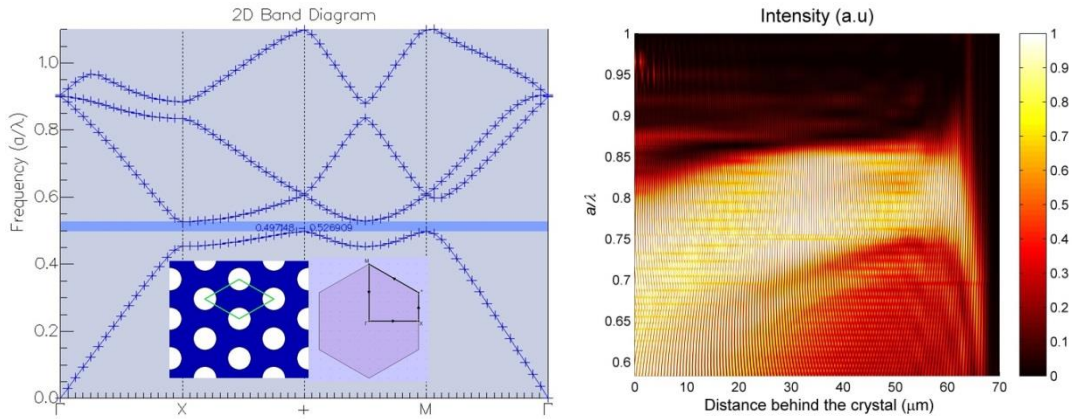

Figure 10. Photonic band diagram for triangular structure and in small, the structure and Brillouin Zone. Representation of frequencies in function of distance behind the crystal at x=0.

4. Numerical Aperture

For this part we need to introduce concepts like a Gaussian width (Fig 11) and the relations of a Gaussian beam propagation in a medium (Eq 5). The width is defined through the amplitude decrease ($1/e^{-2}$) in intensity profile.

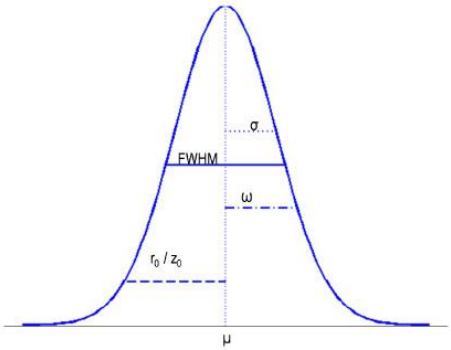

Figure 11. Gaussian beam representation where indicates different important parameters, for us the most important is the width (ω).

The width changes when a Gaussian beam is propagated in a medium as:

$$\omega(z) = \omega_0\sqrt{1 + \frac{z^2}{{z_0}^2}} \tag{5}$$

Where ω_0 is the initial width, z is the distance displaced and $z_0 = {}^{\pi\omega_0^2}/_{\lambda}$ is the Rayleigh distance, where λ is the wavelength.

In order to see how the width of the beam change when pass through a PhC, first we take the intensity profile in the horizontal axis (x=0) (Fig 6, Fig 12a) and search where are the maximum of intensities, in these points take the vertical profile and analyze the width of the beam (Fig 12b, 12c).

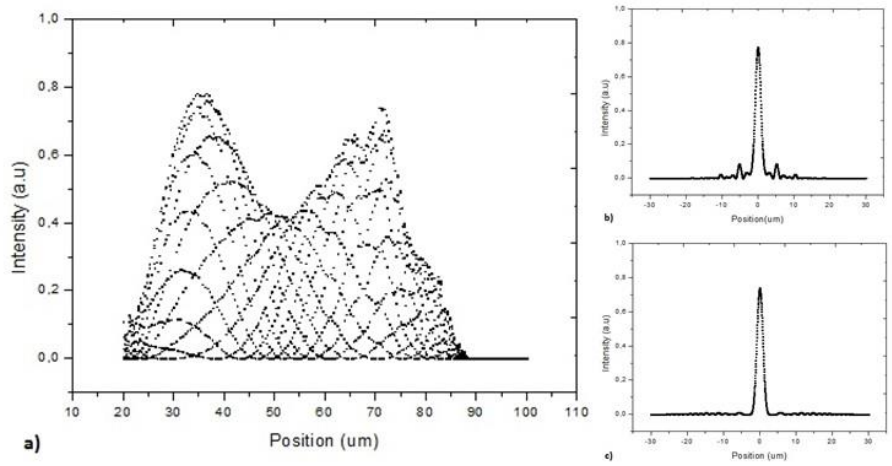

Figure 12. Representation of intensity for input beam with width equal 2µm and frequency (a/λ=0.9). a) Represents the values for intensity in the horizontal axis (x=0) obtaining for the sensor (Sh) (Fig 6), b) Is the vertical profile which was obtaining for sensor (Sv1) in first focal point, c) Is the same that 'b' but with sensor (Sv2) in second focal point.

We did this for several widths of incident Gaussian beam. The Figure 13 represents the diameter or two times the width of the beam in the focal point in function of the diameter of input beam. We can see that for diameters of 1µm to 4µm is possible to obtain double focusing but for 4.5µm to 8µm only obtain one focusing point. The reason is that the central part between the two focusing points (Fig 12a) increase when increase the diameter of the input beam until the central part is bigger than the two focusing points, and starts to disappear and the unique focal point is in the middle.

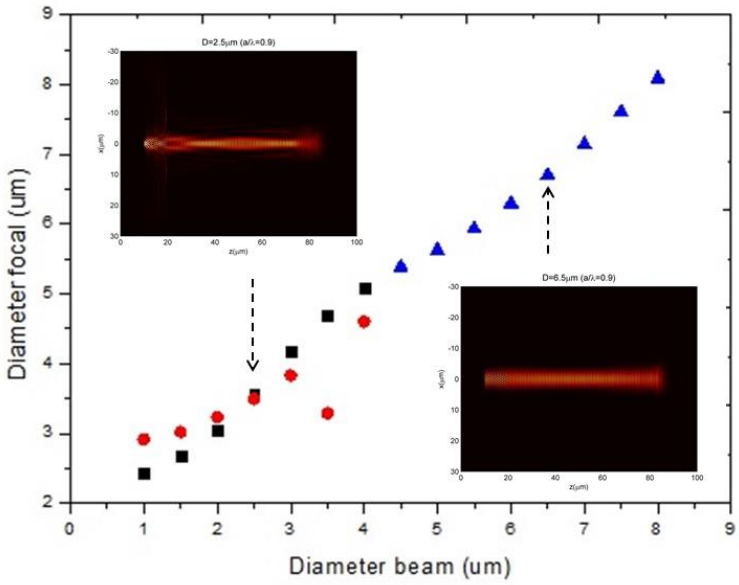

Figure 13. Representation of Gaussian beam diameter in the focal point in function of the Gaussian beam diameter in the input beam. Frequency of the beam (a/λ = 0.9).

If we analyze the Eq 5, we can see that if we maintain the z constant the values of $\omega(z)$ grow up faster for small values of ω_0 and for big ω_0 grow up linearly. Also is possible reduce this equation if we consider $z>>z_0$ and the first term in the square root is neglected. If we do this we obtain:

$$\omega(z) = \frac{\lambda}{\pi\omega_0} z \qquad (6)$$

If we define $\theta = \frac{\lambda}{\pi\omega_0}$ how an angle and in this case is equal to Numerical Aperture (NA).
Now we see what happens with the beam when passes through the PhC. In the focusing point the value of the width is proportional to the NA for small ω_0.

$$\omega' = \frac{\lambda}{\pi NA} \tag{7}$$

The reason for this is because how we saw before the structure of the PhC creates iso-frequency diagrams with different shapes, for some frequency we have a convex shape with a specific dimensions and radius. For this reason, only the part of the beam passes between this width of the convex shape will produce a focusing point and all the other part spread in the normal form. This occurs for small ω_0 because how we explained before the ω(z) grow up faster and great part of the beam doesn't pass for the width of the convex shape.
For big ω_0 the relation is the following:

$$\omega' = \omega_0 \tag{8}$$

Because ω(z) it grows up linearly and is possible to most of the part of the beam pass through the width of the convex shape.
If we consider these two parts, we obtain the following equation. And with this equation is possible to obtain the NA of the photonic crystal through the relation:

$$\omega'^2 = \left(\frac{\lambda}{\pi NA}\right)^2 + \omega_0^2 \tag{9}$$

Using our numerical data we will find the value of NA. First we need to plot the values of ω' versus ω_0, a to fit the data by (9) (wee the Fig 14).

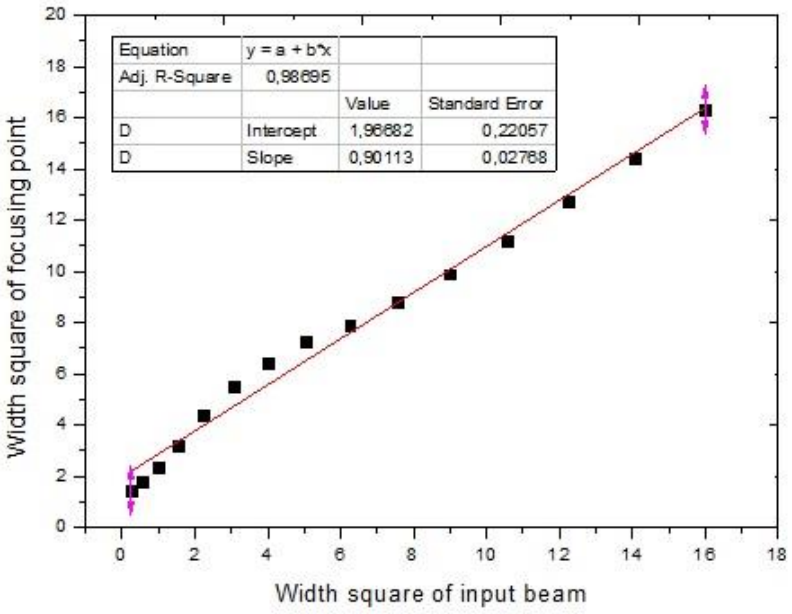

Figure 14. Graphic of width square of focusing point in function of width square of input beam.

From the Figure 14 we confirm that the slope of the line is near to 1, and we find the value of NA using the Equation 9, which is for this specific case (fixed geometry and focal distance) is: $NA = 0.177$

5. Conclusions

In this work we explored several aspects of the beam propagation in PhC in regimes of flat lensing. We simulated structures of two different geometries. We showed first the possibility to obtain a double focusing point in some frequency ranges. We interpreted the self-collimation and flat lensing in terms of iso-frequency lines, and explored the ranges of frequency where the phenomena occur.

One of the importances of the flat lensing by the PhCs is their technological applications in the micro and nano-devices, where the use of the usual lenses is very difficult.

Acknowledgments

I thank to my advisor Kestutis Staliunas for help me to understand several things about this topic. As well as I would want to thank to Lina Maigyte for help me in all the simulation and programing part.

References

[1] C. Cojocaru, L. Maigyte, J. Trull, M. Peckus, M. Malinauskas, K. Staliunas *Double Imaging behind a Woodpile Photonic Crystal* (Universitat Politècnica de Catalunya)

[2] L. Maigyte, *et al*.: Signatures of light-beam spatial filtering in a three-dimensional photonic crystal, *Phys. Rev. A,* vol. 82, 043819-043823(2010).

[3] K. Staliunas and R. Herrero, Nondiffractive propagation of light in photonic crystal, *Phys. Rev. E,* vol. 73. pp. 016601-016606, 2006.

[4] I. Pérez-Arjona, Theoretical prediction of the nondiffractive propagation of sonic waves through periodic acoustic media, *Phys. Rev. B,* vol. 75. pp. 014304-014310, 2007.

[5] V. Espinosa, Subdiffractive propagation of ultrasound in sonic crystals, *Phys. Rev. B,* vol. 76. pp. 140302(R)-140315, 2007.

[6] J. Trull, Formation of collimated beams behind the woodpile photonic crystal, *Phys. Rev. A,* vol. 84. pp. 033812-033816, 2011.

[7] L. Maigyte, C. Cojocaru, V. Purlys, J. Trull, D. Gailevicius, M. Peckus, M. Malinauskas, K. Staliunas, *Focusing by a flat woodpile 3D photonic crystal*, The European Conference on Lasers and Electro-Optics, ISBN: 978-1-4799-0594-2, May 12-16, 2013.

[8] L. Maigyte, V. Purlys, J. Trull, M. Peckus, C. Cojocaru, D. Gailevicius, M. Malinauskas, K. Staliunas, Flat lensing in the visible frequency range by woodpile photonic crystals, *Optics Letters,* vol. 38. Nº.14, July 15, 2013.

[9] L. Maigyte, C. Cojocaru, J. Trull, M. Peckus, V. Mizeikis, M. Malinauskas, M. Rutkauskas, S. Juodkazis, K. Staliunas, *Collimation and Imaging behind a Woodpile Photonic Crystal*, Transparent Optical Networks (ICTON), 2012 14th National Conference.

[10] W. T. Lu and S. Sridhar, *Flat lens without optical axis: Theory of imaging,* 13, 10673 (2005)